

# Photoinduced Charge Transfer between Tetracyano-Anthraquino-Dimethane Derivatives and Conjugated Polymers for Photovoltaics

Gerald Zerza,<sup>\*,†</sup> Markus C. Scharber, Christoph J. Brabec, and N. Serdar Sariciftci

Physical Chemistry, Johannes Kepler University Linz, Altenbergerstrasse 69, A-4040 Linz, Austria

Rafael Gómez, José L. Segura, and Nazario Martín<sup>\*,‡</sup>

Departamento de Química Orgánica, Facultad de Química, Universidad Complutense, 28040 Madrid, Spain

Vojislav I. Srdanov

Institute for Polymers and Organic Solids, University of California, Santa Barbara, California 93106

Received: February 24, 2000; In Final Form: May 28, 2000

The photoinduced charge transfer between tetracyano-anthraquino-dimethane (TCAQ) derivatives and poly[2-methoxy-5-(3,7-dimethyloctyloxy)-1,4-phenylenevinylene] (MDMO-PPV) has been studied by photoinduced absorption (PIA) spectroscopy in the VIS and IR spectral region and by light induced electron spin resonance (LESR). Studies on three different TCAQ derivatives with different side chain substitutions are reported. Among them a supermolecule with TCAQ attached to a fullerene have been synthesized to serve as tandem electron acceptor. The photoinduced absorption in the Vis/near-IR range shows a broad plateau around 1.8 eV followed by two peaks at 1.35 and 1.24 eV with an additional broad feature below 0.5 eV for all three acceptors in composite with MDMO-PPV. All PIA features have a power law excitation intensity dependence with an exponent close to 0.5 as expected for bimolecular kinetics. LESR studies show one absorption at a *g*-factor of 2.0028 with a width (peak-to-peak) of 3.5 G, originating from TCAQ anion radical and the polymer cation radical. Evidence for the formation of a C<sub>60</sub> anion was found in the case of electron transfer from the MDMO-PPV polymer to the TCAQ-C<sub>60</sub> acceptor dyade from these LESR studies. Finally bulk-heterojunction type thin film structures of MDMO-PPV as donor and the TCAQ derivatives as acceptor have been fabricated and tested as photovoltaic devices.

## 1. Introduction

Light induced charge transfer from conjugated polymers and their oligomers to different tetracyano-p-quinodimethane (TCNQ) derivatives and fullerenes has been studied extensively.<sup>1–4</sup> From timeresolved photoinduced absorption (PIA) studies it is well-known that the charge-transfer process from a conjugated polymer to C<sub>60</sub> takes place on an ultrafast time scale (<100fs).<sup>2</sup> On the other hand the back electron transfer is remarkably slow; lifetimes of the order of milliseconds can be observed for the charge separated states in such systems. This very efficient charge separation has been utilized in polymeric photovoltaic devices.<sup>5–11</sup>

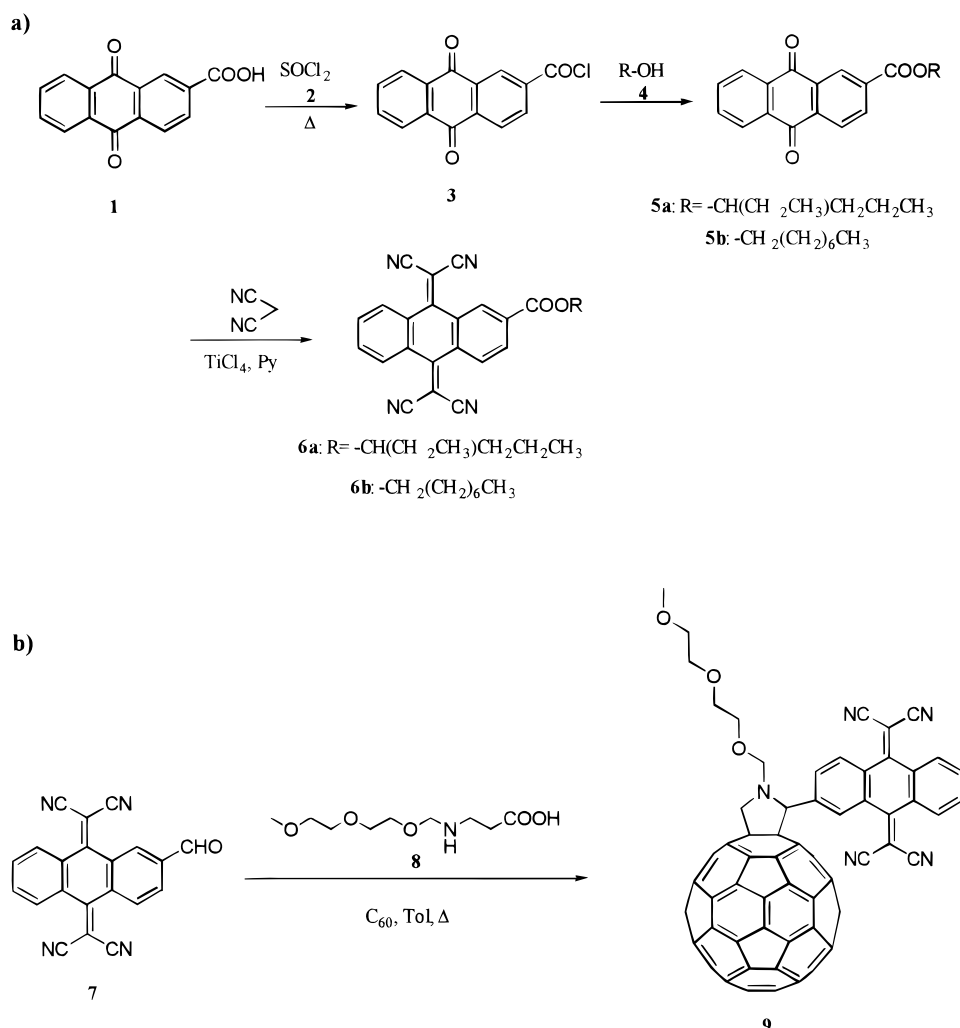
Photoexcitation of oligothiophenes in liquid or solid solutions across the  $\pi$ - $\pi^*$  energy gap produces a metastable triplet state by intersystem crossing from the excited singlet manifold.<sup>12–17</sup> These triplet states were identified by their dipole allowed T<sub>1</sub>-T<sub>2</sub> transition, which exhibit a red shift with increasing chain length.<sup>17</sup> The lifetimes of these triplet states are of the order of 10–100 ms. Electron spin resonance studies of end-capped oligothiophenes in toluene matrices give an unambiguous proof of the triplet character of these excited states.<sup>18</sup> Steady-state photoinduced absorption (PIA) studies on mixtures of oligothiophenes with fullerenes in solutions at room temperature have shown both triplet-triplet energy transfer from the thiophenes

to the fullerene molecules as well as formation of charged species in solvents with high electron affinity.<sup>1</sup> Replacing the acceptor by tetracyanoethylene (TCNE), which has a triplet state higher in energy than the triplet of the oligomer, favored the electron transfer from the triplet state of the oligothiophene to TCNE.

Various PIA studies on thin films of pristine conjugated polymers have also shown the formation of the triplet state after photoexcitation. In composite films of these polymers mixed with electron accepting molecules the triplet absorption is quenched due to charge transfer. Absorption detected magnetic resonance (ADMR) experiments on films of pristine poly[2-methoxy-5-2'-ethylhexyloxy)-1,4-phenylenevinylene] (MEH-PPV) have shown that the origin of the photoinduced absorption in the range between 1.1 and 1.6 eV is due to excited triplet states (spin 1), whereas mixed films of MEH-PPV and C<sub>60</sub> show in the same energetic region features due to charge separated states of spin 1/2.<sup>19</sup> Light induced electron spin resonance (LESR) studies on mixed films of poly[2-methoxy-5-(3,7-dimethyloctyloxy)-1,4-phenylenevinylene] (MDMO-PPV) and a C<sub>60</sub> derivative 1-(3-methoxycarbonyl)-propyl-1-phenyl-(6,6)C<sub>61</sub> (PCBM) showed two light induced ESR lines, one with a *g*-factor of 2.0025 being due to the polymer radical cation and the other one with a *g*-factor 1.9995 originating from the fullerene radical anion.<sup>20</sup> The authors observed the saturation of the polymer-line already at low microwave powers (<1 mW), whereas they could not see any saturation effects on the PCBM

<sup>†</sup> E-mail: Gerald.Zerza@jk.uni-linz.ac.at.

<sup>‡</sup> E-mail: Nazmar@eucmax.sim.ucm.es.

**SCHEME 1: Synthesis and Chemical Structures of the Three TCAQ-type Electron Acceptors (a) 6a,b and (b) 9**

ESR-line up to 200 mW. They concluded that this is due to different spin–lattice relaxation times of the two spins on the polymer and the fullerene.

In another study different TCNQ derivatives were tested with respect to their charge-transfer efficiency to conjugated polymers.<sup>4</sup> Both the amount of luminescence quenching and the PIA signal of the charged states were investigated for two conjugated polymers (MEH–PPV and poly[3-(2-(3-methoxy)ethyl) thiophene] (P3MBET)) and TCNQ derivatives as electron acceptors with different electron affinity. The light induced electron transfer was observed to depend on the electron affinity of the acceptor. Tetracyano-anthraquinone (TCAQ) was found to be a more efficient electron acceptor than TCNQ despite its lower electron affinity.

In this work TCAQ derivatives with alkyl side chain substitutions were prepared, one of them attached to a C<sub>60</sub> molecule forming the acceptor dyad **9** as shown in Scheme 1. The alkyl side chains should provide better solubility in organic solvents and also prevent phase separation between polymer and the electron acceptor. The photoinduced charge transfer from poly[2-methoxy-5-(3,7-dimethyloctyloxy)-1,4-phenylenevinylene] (MDMO–PPV) to these acceptors was studied using PIA in the VIS/NIR and IR range as well as LESR. This photoinduced charge transfer in composite films has been utilized to fabricate bulkheterojunction photovoltaic devices. The results show that these materials have encouraging performance

in photovoltaic energy conversion and might candidate for substitution of the fullerenes commonly used in these devices.<sup>21,22</sup>

## 2. Experimental Section

**2.1. Preparation of the TCAQ Derivatives.** All melting points were measured with a electrothermal melting-point apparatus and are uncorrected. FTIR spectra were recorded as KBr pellets with a Shimadzu FTIR 8300 spectrometer. UV–vis spectra were recorded with a Hewlett-Packard-8452A instrument. <sup>13</sup>C- and <sup>1</sup>H NMR spectra were recorded with a Bruker AC-200 spectrometer (200 MHz and 50 MHz for <sup>1</sup>H and <sup>13</sup>C respectively). Chemical shifts are given as  $\delta$  values (internal standard: TMS). MS were recorded with a Finnigan 8430 (70 eV) spectrometer. Cyclic voltammetric measurements were performed with an EG & PAR Versastat potentiostat using 250 Electrochemical Analysis software. A Metrohm 6.0840.C10 glassy carbon electrode was used as indicator electrode in voltammetric studies. 2-(Hydroxymethyl)-9,10-anthraquinone and 2-carboxy-9,10-anthraquinone are commercially available and were used without further purification.

The preparation of the novel acceptor molecules was carried out by reaction of malonitrile with the respective quinones (**5a,b**) using Lehnert's reagent.<sup>23</sup> The starting quinones were in turn prepared in two steps from the commercially available 2-carboxy-9,10-anthraquinone (**1**) by reaction with thionyl chloride

and further reaction of the formed acid chloride (**3**) with the respective alcohol (**4**) to afford compounds **5a,b** bearing long alkyl chains (Scheme 1).

On the other hand, fulleropyrrolidine **9** was prepared from the previously reported 2-formyl-11,11,12,12-tetracyanoanthraquinodimethane (**7**)<sup>24</sup> and the polyether containing glycine (**8**)<sup>25</sup> by reaction with C<sub>60</sub> in hot toluene. Organofullerene **9** is obtained by cycloaddition reaction of the in situ formed azomethyne ylide to C<sub>60</sub> according to Prato's procedure.<sup>26</sup>

**Synthesis of 2-Alkoxy carbonyl-9,10-anthraquinones (5). General Procedure.** Ten milliliters (140 mmol) of thionyl chloride (**2**) and one gram (4 mmol) of 1,4-anthraquinone-2-carboxylic acid (**1**) were refluxed under argon for 6 h (Scheme 1). After this time, the reaction was allowed to cool at room temperature and the excess of thionyl chloride was removed under vacuum to yield the corresponding acid chloride **3** which was used in the next synthetic step without further purification.

Five milliliters (40 mmol) of the corresponding alcohol **4** were added to the above obtained acid chloride **3** and afterward 0.8 mL (10 mmol) of dry pyridine were added dropwise and the mixture was heated at 100 °C for 5 h. After this time, the solution was cooled in an ice bath and then 10 mL of a 1 M HCl solution were carefully added. The mixture was extracted several times with ethyl ether; the combined organic layers were washed first with saturated NaHCO<sub>3</sub> solution and finally with water. After drying the organic layer with magnesium sulfate, the diethyl ether was removed under vacuum and the excess of alcohol was eliminated by vacuum distillation. The residue obtained was purified by flash chromatography (silica gel, hexane:ethyl acetate).

**2-(1'-Ethylbutoxycarbonyl)-9,10-anthraquinone (5a).** By following the general procedure and using 3-hexanol as the alcohol, **5a** was obtained in a 80% yield, mp 69–71 °C. <sup>1</sup>H NMR (CDCl<sub>3</sub>, 200 MHz) δ 8.86 (s, 1H), 8.40–8.21 (m, 4H), 7.81–7.72 (m, 2H), 5.10 (q, 1H), 1.72–1.28 (m, 6H), 0.94–0.81 (m, 6H). <sup>13</sup>C NMR (CDCl<sub>3</sub>, 50 MHz) δ 182.5, 182.3, 164.8, 135.9, 135.8, 134.5, 134.4, 134.3, 133.5, 133.4, 133.3, 128.4, 127.4, 127.4, 127.3, 77.2, 36.3, 27.7, 18.3, 13.9, 9.3 ppm. FTIR (KBr) ν 2962, 2935, 1718, 1680, 1591, 1460, 1330, 1269, 1246, 1171, 933, 702 cm<sup>-1</sup>.

**2-(Octyloxycarbonyl)-9,10-anthraquinone (5b).** By following the general procedure and using *n*-octanol as the alcohol, **5b** was obtained in a 80% yield, mp 82 °C. <sup>1</sup>H NMR (CDCl<sub>3</sub>, 200 MHz) δ 8.87 (s, 1H), 8.39–8.22 (m, 4H), 7.81–7.72 (m, 2H), 4.33 (t, 2H), 1.75 (q, 2H), 1.24 (s, 10H), 0.81 (t, 3H). <sup>13</sup>C NMR (CDCl<sub>3</sub>, 50 MHz) δ 182.5, 182.3, 165.0, 135.9, 135.5, 134.5, 134.4, 134.3, 133.5, 133.4, 133.3, 128.5, 127.5, 127.4, 127.3, 66.0, 31.7, 29.2, 29.1, 28.6, 25.9, 22.6, 14.0. FTIR (KBr) ν 2951, 2932, 2856, 1724, 1672, 1591, 1475, 1277, 1244, 1173, 949, 708 cm<sup>-1</sup>.

**Synthesis of 2-alkoxy carbonyl-9,10-anthraquinodimethanes (6). General Procedure.** To a refluxing solution of 1.8 mol of the corresponding ester (**5**) in dry chloroform were added, under argon atmosphere, 297 mg (4.5 mmol) of malononitrile, 0.5 mL of TiCl<sub>4</sub> (4.6 mmol), and 0.7 mL (8.75 mmol) of dry pyridine. The reaction was kept under reflux for 72 h, and every 24 h similar amounts of malononitrile, pyridine, and titanium tetrachloride were added. After this time the reaction was allowed to cool at room temperature and then it was poured on a water-ice mixture. The mixture was extracted twice with chloroform; the combined organic layers were washed with water and dried over magnesium sulfate. After removing the solvent under vacuum, the corresponding TCAQ derivative was obtained.

**2-(1'-Ethylbutoxycarbonyl)-11,11,12,12-tetracyanoanthraquin-**

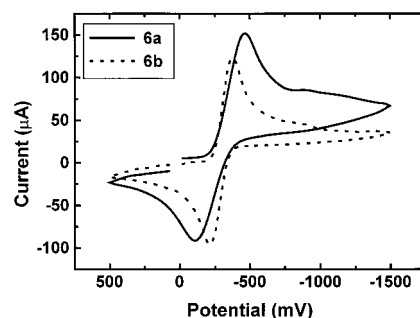


**Figure 1.** Cyclic voltammogram of **6a,b** in dichloromethane and of **9** in toluene:acetonitrile 4:1 with tetrabutylammonium perchlorate as electrolyte and glassy carbon as working electrode and SCE as reference at room temperature.

odimethane (**6a**). The crude product obtained following the above general procedure was purified by crystallization on acetonitrile to afford the pure product in a 48% yield, mp 296–298 °C. <sup>1</sup>H NMR (CDCl<sub>3</sub>, 200 MHz) δ 8.84 (s, 1H), 8.34–8.15 (m, 4H), 7.75–7.66 (m, 2H), 5.08 (q, 1H), 1.74–1.55 (m, 4H), 1.38–1.18 (m, 2H), 0.93–0.78 (m, 6H). <sup>13</sup>C NMR (CDCl<sub>3</sub>, 50 MHz) δ 163.3, 159.2, 134.3, 133.3, 133.0, 132.7, 132.6, 130.4, 130.1, 130.0, 128.3, 127.8, 127.7, 127.6, 112.8, 112.6, 77.8, 35.6, 26.9, 18.5, 13.9, 9.53. FTIR (KBr) ν 2966, 2933, 2228, 1716, 1570, 1458, 1267, 1205, 1107, 758 cm<sup>-1</sup>. MS *m/z* (%I) 406 (4), 331 (33), 306 (100), 278 (12), 251 (12), 224 (7), 207 (15). Cyclic voltammetry (CH<sub>2</sub>Cl<sub>2</sub>): working electrode, glassy carbon; reference electrode, calomel; supporting electrode, Bu<sub>4</sub>NClO<sub>4</sub>. *E*<sup>1/2</sup><sub>red</sub> = -0.291 V (2e). UV-vis (CH<sub>2</sub>Cl<sub>2</sub>) λ(nm) 236, 290, 312, 348.

**2-(Octyloxycarbonyl)-11,11,12,12-tetracyanoanthraquinodimethane (6b).** The crude product obtained following the above general procedure was purified by flash chromatography (silica gel, hexane:ethyl acetate) to afford the pure product in a 75% yield, mp 86–90 °C. <sup>1</sup>H NMR (CDCl<sub>3</sub>, 200 MHz). δ = 8.83 (s, 1H), 8.33–8.17 (m, 4H), 7.75–7.66 (m, 2H), 4.32 (t, 2H), 1.73 (q, 2H), 1.23 (s, 10H), 0.82 (t, 3H). <sup>13</sup>C NMR (CDCl<sub>3</sub>, 50 MHz). δ = 163.8, 158.2, 134.0, 133.3, 132.9, 132.7, 132.6, 130.4, 130.0, 129.8, 128.3, 127.7, 127.6, 112.6, 66.4, 31.7, 29.1, 29.0, 28.5, 25.8, 22.5, 14.0. FTIR (KBr) ν 2926, 2855, 2228, 1722, 1560, 1466, 1329, 1294, 1203, 1178, 1128, 771, 692 cm<sup>-1</sup>. MS *m/z* (%I) 460 (5), 434 (16), 348 (28), 331 (38), 323 (100), 306 (17), 279 (34), 251 (27), 224 (15), 112 (32), 84 (45), 69 (69), 55 (63). Cyclic voltammetry (CH<sub>2</sub>Cl<sub>2</sub>): working electrode, glassy carbon; reference electrode, calomel; supporting electrode, Bu<sub>4</sub>NClO<sub>4</sub>. *E*<sup>1/2</sup><sub>red</sub> = -0.293 V (2e). UV-vis (CH<sub>2</sub>Cl<sub>2</sub>) λ(nm) 236, 290, 312, 350.

**Synthesis of N-(3,6,9-Trioxadecyl)-2-[2'-(11,11,12,12-tetracyanoanthraquinodimethane)] pyrrolidino[3,4:1,2][60]fullerene (9).** To a solution of 144 mg (0.19 mmol) of C<sub>60</sub> in 78 mL of toluene were added 63 mg (0.19 mmol) of the TCAQ-carboxaldehyde **7**<sup>23</sup> and 208 mg (1 mmol) of *N*-(3,6,9-trioxadecyl)glycine (**8**).<sup>24</sup> The mixture was heated to reflux for 48 h, brought to room temperature, poured on top of a silica gel column, and eluted with toluene-ethyl acetate to obtain a black solid which was washed with hexane and diethyl ether (Scheme 1b). Yield 25%. <sup>1</sup>H NMR (CDCl<sub>3</sub>, 200 MHz) δ 8.73 (s, 1H), 8.19–8.34 (m, 3H), 7.78–7.69 (m, 2H), 7.39–7.37 (s, 1H), 5.36 (s, 1H), 5.28 (d, 1H), 4.39 (d, 1H), 3.79–3.55 (m, 10H), 3.36 (s, 3H). <sup>13</sup>C NMR (CDCl<sub>3</sub>, 50 MHz) δ 159.7, 153.8, 152.2, 147.4, 147.3, 146.2, 146.1, 146.0, 145.8, 145.5, 145.2, 146.2, 144.8, 144.5, 144.3, 143.5, 143.5, 143.3, 143.2, 142.6, 142.2, 142.0, 141.8, 140.3, 139.4, 136.3, 135.5, 133.5, 133.1, 132.5, 132.5, 130.1, 129.0, 128.2, 128.1, 127.8, 127.7, 113.0, 83.3,

81.6, 77.2, 75.8, 72.0, 70.6, 69.3, 67.5, 59.1, 52.4. FTIR(KBr)  $\nu$  2950, 2878, 2223, 1198, 1105, 762, 726  $\text{cm}^{-1}$ . Cyclic voltammetry (toluene:acetonitrile 4:1): working electrode, glassy carbon; reference electrode, calomel; supporting electrolyte,  $\text{Bu}_4\text{NClO}_4$ .  $E^1_{\text{red}} = -0.40$  V ( $2e^-$ ),  $E^2_{\text{red}} = -0.65$  V,  $E^3_{\text{red}} = -1.03$  V,  $E^4_{\text{red}} = -1.66$  V,  $E^5_{\text{red}} = -2.17$  V. UV-vis ( $\text{CH}_2\text{-Cl}_2$ )  $\lambda(\text{nm})$  240, 262, 274, 288, 316, 440.

**2.2. Experimental Setup for Charge-Transfer Studies.** The MDMO-PPV polymer was delivered by Covion, Inc., and used as received. For LESR studies samples were prepared as films on a KBr powder. A weight ratio of 1:1 between polymer and the acceptor material was dissolved in toluene in a concentration of 1 mg/mL. The solution was dropped on KBr powder and dried under vacuum before being filled in the ESR-tubes. These samples were placed in the high-Q-cavity of a X-band ESR spectrometer and illuminated with 488 nm light of an Ar-ion laser. The samples were irradiated during the run of the ESR spectra and light off spectra were taken directly afterward to be subtracted from the former one to compensate for the persistent charges produced in the samples. For PIA studies in the VIS/NIR spectral region the samples were prepared as solution cast films on glass substrates using a weight ratio of 4:1 between the polymer and the electron acceptors (**6a,b** and **9** in Scheme 1) and a concentration of 1 mg/ml sample in toluene. PIA spectra were taken using an Ar-ion laser at 488 nm as a pump (typically 40 mW on a 4 mm diameter spot). Using mechanical modulation of the pump beam at 132 Hz, the changes in the white light (120W tungsten-halogen lamp) probe beam transmission ( $-\Delta T$ ) were detected after dispersion with a 0.3 m monochromator in the range from 0.55 to 2.1 eV with a Si-InGaAsSb sandwich detector and recorded phase sensitively with a dual-phase lock-in amplifier. The probe light transmission (T) was recorded separately using the same chopper frequency. From this the PIA spectra ( $-\Delta T/T \approx \Delta\alpha d$ ) are obtained after correction for the sample luminescence and normalization on the probe light transmission.

Infrared activated vibrational (IRAV) spectra are taken using a Bruker IFS 66/S spectrometer with a liquid nitrogen cooled MCT detector. The samples were prepared by drop casting from the mixed polymer/acceptor molecules solution on pressed KBr pellets. Spectra were recorded by 200 accumulations of 10 dark and 10 illuminated cycles. All measurements for LESR, PIA-VIS/NIR and IRAV spectra are done at liquid nitrogen temperature and under vacuum better than  $10^{-5}$  mbar.

Photovoltaic devices were produced by sensitizing MDMO-PPV with **9** and **6b** respectively (Scheme 1). Results were compared to reference photovoltaic devices with an active layer consisting either of pristine MDMO-PPV or MDMO-PPV sensitized with 1-(3-methoxycarbonyl)-propyl-1-phenyl-(6,6)- $\text{C}_{61}$  (PCBM). Preliminary studies showed strong phase separation of TCAQ with MDMO-PPV when spin cast from one solution. These films did not give photovoltaic devices due to large pinholes. Therefore, we used a special production technique, the "bilayer diffusion technique" to produce photovoltaic devices. In this technique, the donor polymer is cast in a first step to give a pinhole free, thin film. In a second step, the acceptor molecule is cast from a solvent or a mixture of solvents that dissolves and/or swells the polymer partially but not completely. During the drying step the acceptor molecules can diffuse into the polymer matrix. Even in the case of a phase separation, this method allows to produce films to fabricate devices. The indium tin oxide (ITO) substrates were covered by a film of poly(3,4-ethylenedioxythiophene)-poly(styrene-sulfonate) (PEDOT) from Bayer AG by doctor blading (see also

Figure 7 in section 3.7). After drying of the PEDOT film, the first layer was cast by doctor blading from a heated solution of MDMO-PPV in toluene. In the second process step, the acceptor molecule (**9**, **6b**, PCBM) was cast from toluene solution. The concentration of the acceptor molecules in solution was varied between 0.25 and 2 wt %. All devices were produced on transparent ITO coated polyester (PET) substrates with 4 cm by 6 cm by doctor blading technique. One substrate carried 36 devices with an active area of 7.5  $\text{mm}^2$  each. The counter electrode was in all cases thermally evaporated aluminum. *I/V* curves were recorded with a Keithley SMU 2400, typically by averaging over 80 measurements for one point. Illumination was provided by white light from a Halogen lamp with 60  $\text{mW}/\text{cm}^2$ .

### 3. Results and Discussion

**3.1. Synthesis.** In contrast to previously reported TCNQ derivatives,<sup>27</sup> the novel compounds prepared exhibit reasonably good solubility in common organic solvents due to the presence of the alkyl chains, thus allowing a full spectroscopic and electrochemical characterization. The UV-vis spectra suggest that these molecules are severely distorted from planarity as has been confirmed by X-ray data for the related unsubstituted 11,11,12,12-tetracyanoanthraquinodimethane (TCAQ).<sup>28</sup> This fact is also supported by the relatively high value for the stretching vibration of the cyano groups which appear at 2230  $\text{cm}^{-1}$  in the IR spectra. In addition, compound **9** shows a typical weak absorption band at 440 nm in the UV-vis spectrum, similar to most dihydrofullerenes. The  $^1\text{H}$  NMR spectrum of **9** shows, in addition to the expected aromatic signals (see Experimental Section), the presence of the pyrrolidine protons at  $\delta$  4.39 and 5.28 as doublets ( $J = 9.9$  Hz; geminal hydrogens) and  $\delta$  5.12 (CH). The  $^{13}\text{C}$  NMR spectrum shows the signals at  $\delta$  83.3, 77.3, 70.0, and 69.2 for the  $\text{sp}^3$  carbons of the pyrrolidine ring and those at the 6,6-ring junction of the  $\text{C}_{60}$  cage.

**3.2. Electrochemistry.** The redox properties of the novel acceptors were studied by cyclic voltammetry at room temperature in dichloromethane for **6a,b** and in toluene 4:acetonitrile 1 for **9** using tetrabutylammonium perchlorate as the supporting electrolyte, glassy carbon as working electrode, and SCE as reference.

Similarly to the parent TCAQ,<sup>29</sup> substituted derivatives **6a,b** show a single-wave, two-electron reduction to the dianion. It has been previously demonstrated that the negative charges in the radical anion and dianion species are mainly located at the two cyanomethylene groups.<sup>30</sup>

Compounds **6a,b** showed the presence of only one reduction wave (**6a**,  $E^{1/2}_{\text{red}} = -0.291$  V; **6b**,  $E^{1/2}_{\text{red}} = -0.293$  V) involving a two-electron process to form the respective dianion species.

Compound **9** showed, in addition to the reduction wave of the TCAQ moiety at  $E^1_{\text{red}} = -0.40$  V ( $2e^-$ ), the presence of four quasi-reversible reduction waves at  $E^2_{\text{red}} = -0.65$  V;  $E^3_{\text{red}} = -1.03$  V;  $E^4_{\text{red}} = -1.66$  V;  $E^5_{\text{red}} = -2.17$  V, (Figure 1) similarly to that found for the parent unsubstituted  $\text{C}_{60}$  [ $-0.60$ ,  $-1.00$ ,  $-1.52$ ,  $-2.04$  V]. It is interesting to note that the first reduction potential of **9** appears cathodically shifted in comparison with **6a,b** which can be accounted for by the electronic effect of the alkoxy carbonyl group in **6a,b**. In addition, the reduction potentials of **9** corresponding to the  $\text{C}_{60}$  moiety are slightly shifted to more negative values related to  $\text{C}_{60}$ . This fact has been explained by the saturation of a double bond of the  $\text{C}_{60}$  core which raises the LUMO energy,<sup>31</sup> and is in good agreement with that found for other fulleropyrrolidines.<sup>32</sup>

**3.3. Light Induced ESR.** No ESR signals could be detected in the pristine MDMO-PPV films neither before nor during

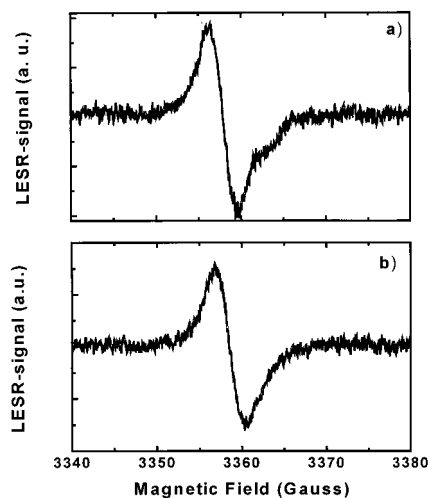


**Figure 2.** LESR signals of (a) MDMO-PPV:**9** and (b) MDMO-PPV:**6b** composite films (weight ratio 1:1) on KBr powder. Illumination at 488 nm, microwave power of 0.2 mW at 100 K.

illumination with 488 nm light. Samples of the pure electron acceptors **9** and **6b** (in Scheme 1) showed a very weak LESR signal consisting of one line with a  $g$ -value 2.0028. Figure 2 shows the LESR spectra of thin films of MDMO-PPV mixed with **9** and **6b**. The estimated weight ratio between polymer and acceptor is 1:1. For both samples an ESR line with  $\Delta H_{p-p}$  3.5 G is observed. The  $g$ -factor has been determined to be 2.0028(3). Switching off the exciting light causes a slow decrease of the so-called “prompt” ESR signal until it stabilizes at a constant value after some 100 s. This so-called “persistent” LESR signal, about one-third of the intensity of the original LESR signal, vanishes only after heating the sample to room temperature. Laser power dependent measurements of the LESR signal show an increase of the LESR signal with laser intensity following a power law with an exponent close to 0.2 and 0.4 for **9** and **6b** composites, respectively. For excitation intensity dependence<sup>34,35</sup> Dyakonov et al. observed a near square root dependence of the LESR signal on the pump power for MDMO-PPV:PCBM composites suggesting bimolecular recombination.<sup>20</sup> In this work for both TCAQ electron acceptors (**9**, **6b**) exponents smaller than 0.5 have been observed.<sup>36</sup>

From ESR studies it is known that the  $g$ -factor of both the TCAQ anion (2.0027(1)) as well as this of the MDMO-PPV polymer cation (positive polaron) (2.0025) are in the range reported here (2.0028(3)).<sup>20,33</sup> So both radicals of the electron donor as well as of the electron acceptor could contribute to the observed LESR signal. Janssen et al. published single broad line LESR spectra of oligothiophenes in solutions containing TCNE as acceptor.<sup>1</sup>

For samples containing the molecule **9** (Scheme 1), which combines the two strong electron acceptors TCAQ and  $C_{60}$ , an additional shoulder like feature is observed in the LESR spectrum at higher fields (Figure 2b) corresponding to a  $g$ -factor close to 2.000. For  $C_{60}$  and  $C_{60}$  derivative anion radicals, a  $g$ -factor close to 2.000 is observed.<sup>20</sup> According to the work of Janssen et al.  $C_{60}$  is more effective photoinduced electron acceptor than TCAQ or TCNQ,<sup>4</sup> despite the higher electron affinity of TCAQ or TCNQ. Following our LESR observations the dominant final state of the electron transferred from the polymer to the electron acceptor dyad can be the TCAQ unit (dominant LESR line) with a small fullerene anion formation (weak LESR shoulder). From these results it seems that both parts of the acceptor dyad are involved in the charge transfer. A stepwise charge transfer, donor  $\rightarrow$  acceptor 1 (fullerene)  $\rightarrow$

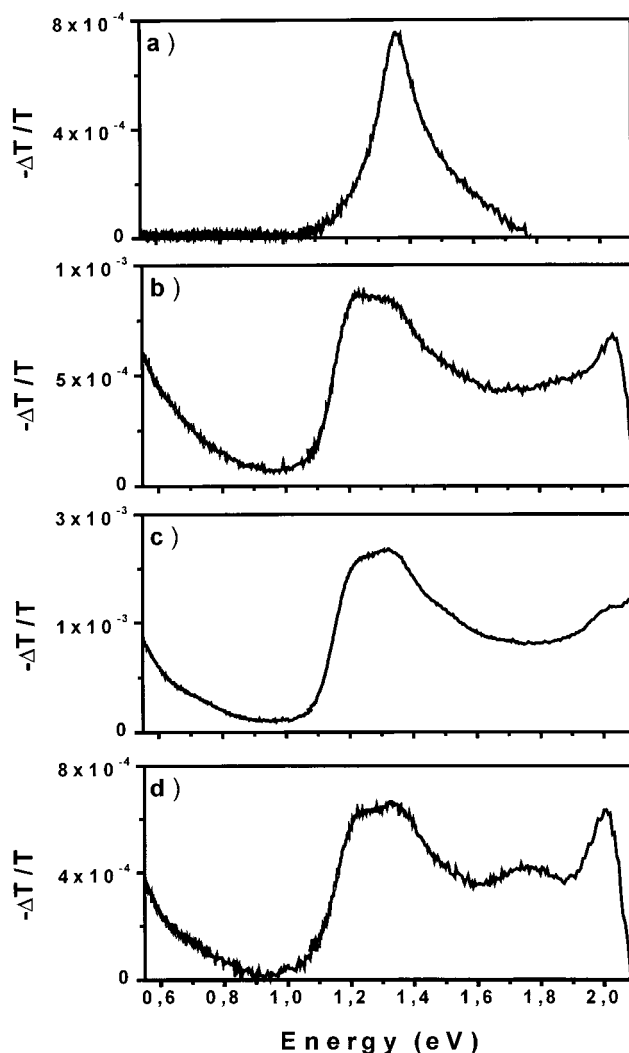


**Figure 3.** Photoinduced absorption spectra of (a) pristine MDMO-PPV film and composite (b) MDMO-PPV:**6a**, (c) MDMO-PPV:**9**, (d) MDMO-PPV:**6b** films. Excitation at 488 nm with 40 mW and 132 Hz modulation,  $T = 100$  K.

acceptor 2 (TCAQ), cannot be excluded by these results. Time-resolved LESR or PIA studies are required to distinguish between direct and stepwise charge transfer.

### 3.4. Photoinduced Absorption (PIA) at VIS/NIR Region.

The photoinduced absorption spectra for a pristine MDMO-PPV film as well as for composite films of MDMO-PPV with the three different TCAQ derivatives are shown in Figure 3. In the case of the pristine MDMO-PPV film a single excited state absorption line at 1.36 eV is observed (Figure 3a). This photoinduced absorption feature is generally associated with the triplet state.<sup>4</sup> Several new PIA features appear in the composite films with **6a**, **9** and **6b** presented in Figure 3b-d. A plateau between 1.9 and 1.4 eV is followed by two closely spaced peaks at 1.24 and 1.33 eV and an additional broad absorption feature lying below 0.5 eV. For all three electron acceptors used, the shape of the PIA spectra is quite similar (Figure 3 b-d). Janssen et al. reported on comparable PIA features for films of MEH-PPV mixed with different TCNQ derivatives.<sup>4</sup> Besides a somewhat higher intensity for the samples containing the fullerene-derivatized supermolecule (Figure 3c), no differences could be observed in the PIA spectra using the three TCAQ type electron acceptors (Figure 3b-d).

The excitation intensity dependencies of the PIA signals are shown in Figure 4. These measurements can give insight into

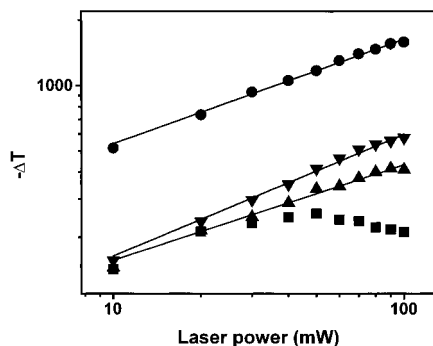


**Figure 4.** Laser power dependence of the photoinduced absorption in Figure 3 for a modulation frequency of 132 Hz: (■) pristine MDMO–PPV (at 1.36 eV), (▼) MDMO–PPV:6a (at 1.24 eV), (●) MDMO–PPV:9 (at 1.24 eV), (▲) MDMO–PPV:6b (at 1.24 eV). The solid lines show fits to a power law dependence.

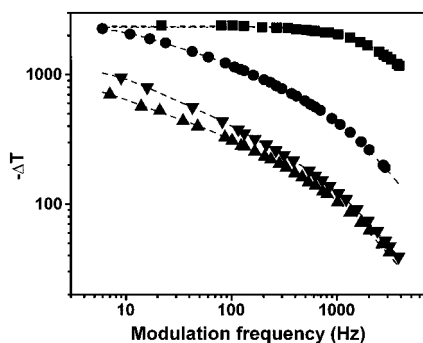


**Figure 5.** Modulation frequency dependence of the photoinduced absorption signal in Figure 3 for 40 mW laser power. (■) pristine MDMO–PPV (at 1.36 eV), (●) MDMO–PPV:9 (at 1.24 eV), (▼) MDMO–PPV:6a (at 1.24 eV), (▲) MDMO–PPV:6b (at 1.24 eV). Dashed lines show fit to monomolecular and bimolecular recombination behavior (see text).

the relaxation kinetics involved in the photoexcited processes. For monomolecular kinetics one predicts a linear increase of the photoproduct with the excitation intensity and for a bimolecular recombination in the low modulation frequency limit ( $\omega\tau \ll 1$ ) a square root dependence.<sup>35,38</sup> For the PIA signals of these donor/acceptor composite films a power law dependence with an exponent close to 0.5 can be extracted from Figure 4. For the pristine MDMO–PPV films on the other hand the observed dependence of the PIA signal on the excitation power does not follow a simple power law (Figure 4). It resembles rather the behavior of a saturated absorption.

Also a modulation frequency  $\omega$  dependent measurement of the PIA signal can give insight into the mechanisms involved in the kinetics of the photoexcited states and give an estimate on the lifetime of the photoproducts.<sup>34,35</sup> Figure 5 shows a comparison of the PIA signals for the pristine MDMO–PPV film (at 1.36 eV) and the mixed films (at 1.24 eV) as a function of the chopping frequency. For the case of pristine MDMO–PPV the signal stays nearly constant up to frequencies of 800 Hz until it decreases remarkably. A fit assuming monomolecular kinetics as given in equation 1

$$\Delta T \propto \sum_i \frac{1}{\sqrt{1 + \omega^2 \tau_i^2}}, \quad i = 1..2 \quad (1)$$

gives good results if at least two lifetime components  $\tau_i$  of the order of 40 and 200  $\mu$ s are assumed.<sup>34</sup> For the composite samples the signal decays by 1 order of magnitude for a frequency

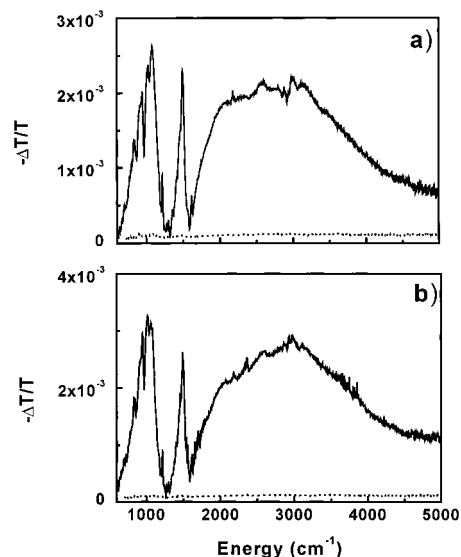


**Figure 6.** Photoinduced IRAV measurements of (a) MDMO–PPV:9 (solid line) and (b) MDMO–PPV:6b (solid line) composite films on KBr. The dotted lines in (a) and (b) show for comparison the IRAV signals for the pristine polymer film. Excitation with 488 nm at  $T = 100$ K.

increase by 2 orders of magnitude (Figure 5), so approximately with  $1/\omega^{0.5}$ . Also shown in Figure 5 are fits of the frequency dependence of the PIA signals (at 1.24 eV) to a bimolecular recombination kinetics as described by Dellepiane et al.<sup>34</sup> However, only a fit with multiple time constants (see eq 2) between 100  $\mu$ s and 30 ms achieved good agreement between the experimental results and the bimolecular model as shown in eq 2:

$$\Delta T \propto \sum_i \frac{\alpha_i \tanh \alpha_i}{\alpha_i + \tanh \alpha_i}, \quad i = 1..3 \quad (2)$$

where  $\Delta T$  is the steady-state PIA signal and  $\alpha_i = \pi/(\omega\tau_i)$  with the modulation frequency  $\omega$  of the exciting laser.

Janssen et al. reported on a similar frequency dependence of their PIA spectra of MEH–PPV films with different TCNQ derivative acceptors.<sup>4</sup> Botta et al. observed a  $1/\omega$  decay of the PIA signal for long-lived charged excitations of polymers in solutions, with only one lifetime involved.<sup>35,38</sup> On the other hand, the  $1/\omega^{0.5}$  dependence of the PIA signal in polymer films, similar as in our case, was attributed to a broad distribution of different lifetimes of trapped charge carriers.

**3.5. Infrared Activated Vibrational (IRAV) Spectra.** A further indication for the charge transfer from the MDMO–PPV to the TCAQ type electron acceptors is by light induced FT IR spectroscopy.<sup>39</sup> The light induced IRAV spectra of pristine MDMO–PPV and MDMO–PPV with 9 and 6b, taken under 488 nm light illumination, are shown in Figure 6. For the pristine polymer no detectable light induced features appear (dotted line in Figure 6). By adding the electron acceptor to the polymer the PIA results in a broad electronic subgap absorption at 3000  $\text{cm}^{-1}$  (0.37 eV) and strong infrared active vibrational bands around 1490  $\text{cm}^{-1}$  (0.185 eV) and 1000  $\text{cm}^{-1}$  (0.125 eV) emerge in Figure 6a,b. These bands corresponds to Raman active modes of the neutral polymer, which become infrared active for the charged species.<sup>39</sup> The broad unstructured absorption around 3000  $\text{cm}^{-1}$  corresponds to the continuation of the low energy polaron feature ( $<0.5$  eV) shown in Figure 3b–d. Brabec et al. reported on IRAV measurements on MEH–PPV with the fullerene derivative PCBM in polystyrene matrices

**TABLE 1: Luminescence Quantum Efficiencies of Pristine and Composite Polymer Films Measured with an Integrating Sphere Setup for 488 nm Excitation at Room Temperature**

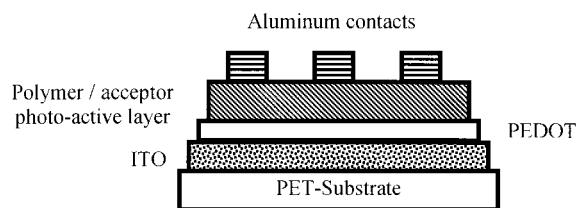
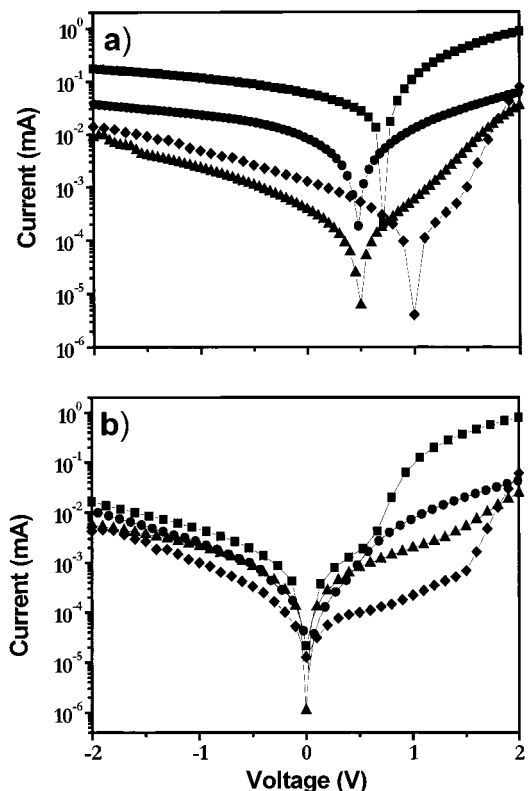
MDMO-PPV pristine	MDMO-PPV:PCBM	MDMO-PPV: <b>9</b>	MDMO-PPV: <b>6b</b>
2.6%	0.3%	0.3%	0.9%

with similar results.<sup>40</sup> Unsubstituted PPV shows light induced IR-absorptions at 1470, 1398, 1274, and 1100  $\text{cm}^{-1}$ .<sup>41</sup> For another substituted PPV derivative, IRAV bands at 1485, 1217, 1086, and 1028  $\text{cm}^{-1}$  have been published.<sup>41</sup>

From excitation intensity dependent measurements of the IR absorption at 1000 and 3000  $\text{cm}^{-1}$  (Figure 6) a sublinear increase with an exponent considerably smaller than 0.5 is observed like in the LESR measurements. Cha et al. showed, from their photoinduced infrared absorption studies on various conjugated polymers, that a bimolecular recombination of polarons formed from polaron pairs can be responsible for such a power law intensity dependence with an exponent smaller than 0.5.<sup>36</sup> According to their calculations in the limit of high excitation intensities a power law dependence with an exponent of 0.25 should be observed.

**3.6. Luminescence Quenching.** To compare the efficiencies for the charge transfer of the different TCAQ acceptors and the fullerene derivative PCBM, the luminescence quantum efficiency of the pristine polymer sample and the mixed polymer/acceptor samples have been determined using an integrating sphere arrangement.<sup>42,43</sup> For all samples a relatively low electron acceptor concentration of 0.1 mol % was used. Table 1 shows a comparison of the luminescence quantum efficiencies for the MDMO-PPV samples with three different electron acceptors mixed inside and excited at 488 nm. The optical density of the samples at the excitation wavelength was determined to be close to 1. The luminescence quantum efficiency of the pristine MDMO-PPV sample is of the order of 3%. Adding 0.1 mol % of PCBM or **9** to the MDMO-PPV quenches the luminescence by a factor of 9, whereas using the same amount of **6b** as acceptor only reduces the MDMO-PPV luminescence by a factor of 3 (Table 1). So there is evidence that those electron acceptors containing the  $\text{C}_{60}$  unit (PCBM and **9**) induce a more efficient luminescence quenching as compared to the pure TCAQ derivative acceptors. Janssen et al. report on a about 4 times higher quenching rate of the MEH-PPV luminescence by  $\text{C}_{60}$  compared to TCAQ.<sup>4</sup> Moreover for the case of the "electron acceptor dyade" **9** composed of a fullerene and a TCAQ unit there seems to be some evidence for an additional influence of the  $\text{C}_{60}$  unit on the electron accepting properties of the whole compound. Though a change in morphology and phase separation of the sample in going from a TCAQ-type to a fullerene-type electron acceptors may also strongly influence the amount of luminescence quenching.

**3.7. Photovoltaic Devices.** We have fabricated donor/acceptor interpenetrating network type photovoltaic devices as published before.<sup>8,21,22</sup> Figure 7 describes the setup of the thin film solar cell devices in a schematic way. Figure 8a,b shows the  $I/V$  curves of photovoltaic devices produced of pristine MDMO-PPV and MDMO-PPV sensitized with **9**, **6b**, and PCBM under illumination with 60  $\text{mW}/\text{cm}^2$  white light and dark, respectively. The highest short circuit currents ( $I_{\text{sc}}$ ) are observed for devices produced from MDMO-PPV with PCBM. The rectification of these devices is up to 100 at  $\pm 2$  V in the dark. The open circuit voltage  $V_{\text{oc}}$  for the device presented is 720 mV, the short circuit current  $I_{\text{sc}} = 60 \mu\text{A}$  for an active area of 0.075  $\text{cm}^2$ . With a filling factor of 0.4 this sums up to a power conversion

**Figure 7.** Schematic setup of a plastic solar cell device. polyester (PET), indium tin oxide (ITO), poly(3,4-ethylenedioxythiophene)-polystyrenesulfonate (PEDOT).**Figure 8.** Current-voltage characteristics of different bulk heterojunction photovoltaic devices of 0.075  $\text{cm}^2$  active area. (a) Under 60  $\text{mW}/\text{cm}^2$  white light illumination and (b) in the dark. (◆) Pristine MDMO-PPV, (■) MDMO-PPV:PCBM, (●) MDMO-PPV:**9**, and (▲) MDMO-PPV:**6b** as photoactive layers.

efficiency of 0.4% for 60  $\text{mW}/\text{cm}^2$  white light. Using **9** instead of PCBM reduced the short circuit currents to 8  $\mu\text{A}$ . Under these illumination conditions  $V_{\text{oc}}$  was measured to be 480 mV with a filling factor of 0.3 which results in a power conversion efficiency of the order of 0.03%. Both, the rectification and the current under forward bias are lower. It is interesting to note that the dark and the illuminated  $I/V$  curve of the device with the electron acceptor **9** are rather symmetric around 0 V and  $V_{\text{oc}}$  respectively. This symmetry might indicate an ohmic contribution to the diode, probably due to small shunts as a consequence of immiscibility between **9** and MDMO-PPV. Also atomic force microscopy (AFM) studies gave evidence of phase separation between the MDMO-PPV and **9**.

The photocurrent and the power conversion efficiency of **6b** are clearly less than for **9** by an order of magnitude. The photophysical investigation presented above gave clear evidence, that photoinduced charge transfer between MDMO-PPV and **6b** occurs. Therefore, the weak photovoltaic performance of MDMO-PPV with **6b** can only be explained by poor charge carrier transport of the electron via **6b**.

#### 4. Conclusions

Photoinduced charge transfer between the MDMO–PPV polymer and three TCAQ derivative electron acceptors has been observed by light induced ESR, photoinduced absorption and luminescence quenching. From the luminescence quenching data it can be stated that fullerenes or fullerene containing derivatives, like the electron acceptor dyade TCAQ-C<sub>60</sub>, are somewhat more efficient quenchers than TCAQ type electron acceptors.

The efficiency of photovoltaic devices based on MDMO–PPV sensitized with TCAQ type acceptors is limited by the phase separation between the donor and the acceptor. Using differently substituted TCAQs giving higher compatibility to PPV type polymers as well as investigations of the photoinduced charge-transfer properties of TCAQs with other classes of conjugated polymers, such as polythiophenes, polyfluorenes is suggested to overcome these phase incompatibility problems.

**Acknowledgment.** This work is supported by the “Fonds zur Förderung der wissenschaftlichen Forschung” of Austria (Project P-12680-CHE) and was also performed within the Christian Doppler Foundations dedicated laboratory on Plastic Solar Cells funded by the Austrian Ministry of Economic Affairs and Quantum Solar Energy Linz GesmbH. The authors also gratefully acknowledge the support of the European Community (Joule III).

#### References and Notes

- Janssen, R. A. J.; Moses, D.; Sariciftci, N. S. *J. Chem. Phys.* **1994**, *101*, 9519.
- (a) Kraabel, B.; Hummelen, J. C.; Vacar, D.; Moses, D.; Sariciftci, N. S.; Heeger, A. J.; Wudl, F. *J. Chem. Phys.* **1996**, *104*, 4267. (b) Brabec, C. B.; Zerza, G.; Sariciftci, N. S.; Cerullo, G.; De Silvestri, S. *Nature*. **2000**. Submitted for publication.
- Sariciftci, N. S.; Smilowitz, L.; Heeger, A. J.; Wudl, F. *Science* **1992**, *258*, 1474.
- Janssen, R. A. J.; Christiaans, M. P. T.; Hare, C.; Martín, N.; Sariciftci, N. S.; Heeger, A. J.; Wudl, F. *J. Chem. Phys.* **1995**, *103*, 8840.
- Sariciftci, N. S.; Braun, D.; Zhang, C.; Srdanov, V.; Heeger, A. J.; Stucky, G.; Wudl, F. *Appl. Phys. Lett.* **1993**, *62*, 585.
- Morita, S.; Zakhidov, A. A.; Yoshino, K. *Jpn. J. Appl. Phys.* **1993**, *32*, L1873.
- Sariciftci, N. S.; Heeger, A. J.; U.S. Patent 5,331,183, July 19, 1994.
- Yu, G.; Gao, J.; Hummelen, J. C.; Wudl, F.; Heeger, A. J. *Science* **1995**, *270*, 1789.
- Halls, J. J. M.; Walsh, C. A.; Greenham, N. C.; Marseglia, E. A.; Friend, R. H.; Moratti, S. C.; Holmes, A. B. *Nature* **1995**, *376*, 498.
- Tada, K.; Hosoda, K.; Hirohata, M.; Hidayat, R.; Kawai, T.; Onoda, M.; Teraguchi, M.; Masuda, T.; Zakhidov, A. A.; Yoshino, K. *Synth. Met.* **1997**, *85*, 1305.
- Tada, K.; Hidayat, R.; Hirohata, M.; Kawai, T.; Lee, S. B.; Bakhadirov, I. U.; Zakhidov, A. A.; Yoshino, K. *Synth. Met.* **1997**, *85*, 1349.
- Wintgens, V.; Valat, P.; Garnier, F. *J. Phys. Chem.* **1994**, *98*, 229.
- Chosrovian, H.; Grebner, D.; Rentsch, S.; Naarman, H. *Synth. Met.* **1992**, *52*, 213.
- Lap, D. V.; Grebner, D.; Rentsch, S.; Naarman, H. *Chem. Phys. Lett.* **1993**, *211*, 135.
- Chosrovian, H.; Rentsch, S.; Grebner, D.; Dahm, D. U.; Birckner, E.; Naarman, H. *Synth. Met.* **1993**, *60*, 23.
- Charra, F.; Fichou, D.; Nunzi, J.-M.; Pfeffer, N. *Chem. Phys. Lett.* **1992**, *192*, 566.
- Janssen, R. A. J.; Smilowitz, L.; Sariciftci, N. S.; Moses, D. *J. Chem. Phys.* **1994**, *101*, 1787.
- Bennati, M.; Grupp, A.; Bäuerle, R.; Mehring, M. *Mol. Cryst. Liq. Cryst.* **1994**, *256*, 751.
- Wei, X.; Vardeny, Z. V.; Sariciftci, N. S.; Heeger, A. J. *Phys. Rev. B* **1996**, *53*, 2187.
- Dyakonov, V.; Zorinaints, G.; Scharber, M.; Brabec, C. J.; Janssen, R. A. J.; Hummelen, J. C.; Sariciftci, N. S. *Phys. Rev. B* **1999**, *59*, 8019.
- Brabec, C. J.; Padinger, F.; Dyakonov, V.; Hummelen, J. C.; Janssen, R. A. J.; Sariciftci, N. S. In *Proceedings of the International Winterschool on Novel Materials*, Kirchberg am Wechsel, Austria, 1997; Kuzmany, H., Ed.; World Scientific Publishing Company: River Edge, NJ, 1998; pp 519–522.
- (a) Brabec, C. J.; Padinger, F.; Hummelen, J. C.; Sariciftci, N. S. *J. Appl. Phys.* **1999**, *85*, 6866. (b) Gebeyehu, D.; Padinger, F.; Brabec, C. J.; Fromherz, T.; Hummelen, J. C.; Sariciftci, N. S. *International Journal of Photoenergy* **1999**, *1*, 89–95.
- Lehnert, W. *Tetrahedron Lett.* **1970**, 4723. Lehnert, W. *Synthesis* **1974**, 667.
- Illescas, B.; Martín, N.; Seoane, C. *Tetrahedron Lett.* **1997**, *38*, 2015.
- da Ros, T.; Prato, M.; Novello, F.; Maggini, M.; Banfi, E. *J. Org. Chem.* **1996**, *61*, 9070.
- Maggini, M.; Scorrano, G.; Prato, M. *J. Am. Chem. Soc.* **1993**, *115*, 9798.
- (a) Martín, N.; Hanack, M. *J. Chem. Soc., Chem. Comm.* **1988**, 1522; Martín, N.; Behnisch, R.; Hanack, M. *J. Org. Chem.* **1989**, *54*, 2563. (b) De la Cruz, P.; Martín, N.; Miguel, F.; Seoane, C.; Albert, A.; Cano, F. M.; González, A.; Pingarrón, J. M. *J. Org. Chem.* **1992**, *57*, 6192. (c) Bando, P.; Martín, N.; Segura, J. L.; Seoane, C.; Ortí, E.; Viruela, P. M.; Viruela, R.; Albert, A.; Cano, F. H. *J. Org. Chem.* **1994**, *59*, 4618.
- Schubert, U.; Hünig, S.; Aumüller, A. *Liebigs Ann. Chem.* **1985**, 1216.
- (a) Aumüller, A.; Hünig, S. *Liebigs Ann. Chem.* **1984**, 618; Kini, A. M.; Cowan, D. O.; Gerson, F.; Möckel, R. *J. Am. Chem. Soc.* **1985**, *107*, 556. (b) Two one-electron waves at  $-0.46$  and  $-0.65$  V in acetonitrile have been also reported for TCAQ. Yamaguchi, S.; Tatemitsu, H.; Sakata, Y.; Misumi, S. *Chem. Lett.* **1983**, 1229.
- (a) Gerson, F.; Heckendorn, R.; Cowan, D. O.; Kini, A. M.; Maxfield, M. *J. Am. Chem. Soc.* **1983**, *105*, 7017. (b) Martín, N.; Seoane, C. In *Handbook of Organic Conductive Molecules and Polymers*; Nalwa, H. S., Ed.; John Wiley & Sons Ltd.: New York, 1997; Vol. 1.
- (a) Suzuki, T.; Muruyama, Y.; Akasaba, T.; Ando, W.; Kobayashi, K.; Nagase, S. *J. Am. Chem. Soc.* **1994**, *116*, 1359. (b) For a recent review, see: Echegoyen, L.; Echegoyen, L. E. *Acc. Chem. Res.* **1998**, *31*, 593.
- Prato, M.; Maggini, M. *Acc. Chem. Res.* **1998**, *31*, 519.
- Kini, A. M.; Cowan, D. O.; Gerson, F.; Möckel, R. *J. Am. Chem. Soc.* **1985**, *107*, 556.
- Dellepiane, G.; Cuniberti, C.; Comoretto, D.; Musso, G. F.; Figari, G.; Piaggi, A.; Borghesi, A. *Phys. Rev. B* **1993**, *48*, 7850.
- Botta, C.; Luzzati, S.; Tubino, R.; Bradley, D. D. C.; Friend, R. H. *Phys. Rev. B* **1993**, *48*, 14809.
- Cha, Y.-H.; Furukawa, Y.; Tasumi, M.; Noguchi, T.; Ohnishi, T. *Chem. Phys. Lett.* **1997**, *273*, 159.
- Fichou, D.; Horowitz, G.; Xu, B.; Garnier, F. *Synth. Met.* **1990**, *39*, 243.
- Botta, C.; Luzatti, S.; Tubino, R.; Borghesi, A. *Phys. Rev. B* **1992**, *46*, 13008.
- Ehrenfreund, E.; Vardeny, Z. V.; Brafman, O.; Horowitz, B. *Phys. Rev. B* **1987**, *36*, 1535.
- Brabec, C. J.; Dyakonov, V.; Sariciftci, N. S.; Graupner, W.; Leising, G.; Hummelen, J. C. *J. Chem. Phys.* **1998**, *109*, 1185.
- Tian, D. B.; Zerbi, G.; Müllen, K. *J. Chem. Phys.* **1991**, *95*, 3198.
- Park, J. Y.; Heeger, A. J.; Srdanov, V. I. 2000. In press.
- Samuel, I. D. W.; Rumbels, G.; Friend, R. H. In *Primary Photoexcitations in Conjugated Polymers: Molecular Excitations versus Semiconductor Band Model*; N. S. Sariciftci, N. S., Ed.; World Scientific Publishing Company: River Edge, NJ, 1997.